Journal of Hydrology 576 (2019) 1–11

Contents lists available at ScienceDirect

Journal of Hydrology

journal homepage: www.elsevier.com/locate/jhydrol

Research papers

Characterization of CDOM in reservoirs and its linkage to trophic status assessment across China using spectroscopic analysis

Yingxin Shang[a,d], Kaishan Song[a,c,*], Pierre A. Jacinthe[b], Zhidan Wen[a], Lili Lyu[a], Chong Fang[a,d], Ge Liu[a]

[a] Northeast Institute of Geography and Agroecology, CAS, Changchun 130102, China
[b] Department of Earth Sciences, Indiana University-Purdue University, Indianapolis, USA
[c] School of Environment and Planning, Liaocheng University, Liaocheng 252000, China
[d] University of Chinese Academy of Science, Beijing 100049, China

ARTICLE INFO

This manuscript was handled by Huaming Guo, Editor-in-Chief

Keywords:
CDOM
FRI-EEM
Inland waters
Eutrophication

ABSTRACT

Chromophoric dissolved organic matter (CDOM) represents the optically active component of the DOM pool, and originates from both allochthonous and autochthonous sources. The fluorescent characteristics of dissolved organic matter (FDOM) has been widely used to trace CDOM sources and infer its composition. However, little is known about the optical and fluorescent properties of CDOM in drinking water reservoirs, and the variability of CDOM properties along trophic gradients in these aquatic systems. A total of 536 water samples were collected between 2015 and 2017 from 131 reservoirs across China to characterize CDOM and FDOM properties using both light absorption and fluorescence spectroscopies, and examine relationships with water-quality condition as expressed by the modified trophic state index (TSI_M) of the reservoirs (range: $12 < TSI_M < 78$). With increased reservoir trophic status, CDOM absorption coefficients at 254 nm ($a_{CDOM}(254)$) and total fluorescence of FRI-EEMs (excitation-emission matrix coupled with fluorescence regional integration) increased significantly ($p < 0.01$). Our results indicated that the nutrients in aquatic systems and the social economy factors (including wastewater, sewage, cultivated land, GDP, population) and altitude affect the CDOM absorption and fluorescence significantly ($p < 0.05$). Most importantly, we proposed a new classification standard associated with eutrophic status via CDOM humification index (HIX) due to the significant correlation between each other ($p < 0.01$). HIX less than 4 was corresponding to TSI_M less than 30 as oligotrophic states; $4 < HIX \leq 12$ was corresponding to TSI_M less than 50 as mesotrophic states; $12 < HIX \leq 18$ was corresponding to TSI_M less than 70 as eutrophic states; HIX more than 18 is defined as hypereutrophic status with $TSI_M > 70$. This method highlights the importance of CDOM fluorescence for aquatic DOM input and strengthens the linkage between the trophic status index and CDOM characteristics, it also contributes to establish a new rapid assessing model with quick experimental measurements to monitor the trophic status of water reservoirs.

1. Introduction

China is the greatest dam-building country in the world and has more than 87,000 reservoirs with a total water storage capacity of 706 billion m^3 (Yang et al., 2012). Reservoirs are important for both economic and social sustainable development, providing a stable supply of water for agricultural, industrial, recreational and residential use (Han, 2010). Nationwide, reservoirs account for a significant amount of the total urban drinking water sources (Vörösmarty et al., 2000). In many parts of the country however, that water supply is threatened by eutrophication, a condition affecting many reservoirs due to high input of nitrogen (N) and phosphorus (P) from domestic sources, and extensive agricultural and industrial activities (Smith and Schindler, 2009). This nutrient enrichment has implications for the trophic state classification of the water reservoir (the trophic state is defined as the total weight of living biomass in a water body at a specific location and time; Dunalska, 2011). The most frequently used parameters for determination of the trophic state of a water body include: concentration of nutrients [total phosphorus (TP) and total nitrogen (TN)] and chlorophyll-a (*Chla*), as well as water clarity expressed as Secchi disk depth (SDD) (Carpenter et al., 1998; Nürnberg 2001). Carlson (1977) and more recently Kratzer and Brezonik (2010) proposed a common classification using a points

* Corresponding author at: Northeast Institute of Geography and Agroecology, CAS, Changchun 130102, China.
E-mail addresses: shangyingxin@neigae.ac.cn (Y. Shang), songkaishan@iga.ac.cn (K. Song), pjacinth@iupui.edu (P.A. Jacinthe), wenzhidan@neigae.ac.cn (Z. Wen), lvlili@neigae.ac.cn (L. Lyu), fangchong@neigae.ac.cn (C. Fang), liuge@neigae.ac.cn (G. Liu).

https://doi.org/10.1016/j.jhydrol.2019.06.028
Received 26 March 2019; Received in revised form 9 June 2019; Accepted 10 June 2019
Available online 12 June 2019

system ranging from 0 to 100 (TSI -Trophic State Index). Laboratory measurements of these parameters can be quite laborious which precludes quick assessment of the trophic state of reservoirs; as a result, trophic state information is generally available at low temporal and spatial resolutions (Zhang et al., 2018). In addition to nutrients availability and primary productivity in aquatic systems, the trophic state can be affected by environmental pollution from anthropogenic activity, by lighting and turbidity conditions, and by the quantity and quality of organic matter present in the water body (Dunalska, 2009). Collection of all these data can be costly and time-consuming. Therefore, there is an urgent need to develop an alternative method to assess the trophic state of water reservoirs using parameters that can be retrieved from optical characteristics of dissolved organic matter (DOM).

Chromophoric dissolved organic matter (CDOM) plays an important role in the ecology of aquatic systems; a high concentration of organic matter in natural waters is generally an indicator of pollution and potential for hypoxia (Zhao et al., 2016). Therefore, knowledge of the sources, composition, and transformation of CDOM would further our ability to monitor and protect the ecological integrity of aquatic systems. The fluorescent CDOM (FDOM) has been widely used to trace CDOM sources, distribution and composition (Zhang et al., 2009, 2010). In that regard, EEM (excitation-emission matrix) coupled with fluorescence regional integration (FRI-EEM) has been a promising quantitative technique that is based on wavelength-dependent paired fluorescence intensity data to define EEM regions, and each integrated fluorescence intensity region represents a specific FDOM component (Chen et al. 2003; Zhao et al., 2017). The development of more sensors related to CDOM fluorescence can facilitate the adoption of FRI-EEM techniques for monitoring of freshwater ecosystems (Liu et al., 2014; Lee et al., 2015; Bowling et al., 2016). Therefore, models can be developed to assess the trophic state of freshwater systems using CDOM fluorescence; this would lead to comprehensive and regular monitoring of water quality in terms of both light condition and nutrients, and ultimately more effective reservoirs management.

According to a national monitoring of reservoirs conducted in 2015, 9.8%, 67.2%, 19.7% and 3.3% of the reservoirs in China were found to be oligotrophic, mesotrophic, light-eutrophic and mid-eutrophic, respectively. Some studies have proposed to assess trophic state using the nutrient-color paradigm, an approach largely based on CDOM absorption and total organic matter (Webster et al., 2008; Dunalska, 2011). However, even though FDOM is a significant part of CDOM, no linkage between FDOM properties and the trophic state has been established for reservoirs in previous studies. Therefore, the main objectives of this study were to: (1) assess CDOM absorption and fluorescence properties and composition changes along trophic gradients (from oligotrophic to eutrophic) in freshwater reservoirs; (2) develop relationships between CDOM properties and trophic state index (TSI_M) of the reservoirs; (3) examine relationships between CDOM fluorescence and altitude, water chemical parameters and socio-economic factors; and (4) discuss potential applications of the FRI-EEM model for assessing and monitoring the trophic state of reservoirs using CDOM fluorescence data.

2. Materials and methods

2.1. Field sampling

A total of 131 reservoirs were selected across China to characterize FDOM features (Fig. 1). In total, 536 water samples were collected mainly between 2015 and 2017. In the northeast part of China, 192 samples were taken from late August 2015 and August 2016. Field campaign was carried out in the eastern part of China and Yungui region of China in October 2015, and 262 samples were collected from 56 reservoirs. For the Inner Mongolia region, 55 samples were taken in early August of 2015. There were 27 samples taken from the Tibetan plateau region during the late of July in 2015 and 2017. During water sampling, geographical coordinates and altitude of each sampling point were recorded with a GPS receiver. Several water-quality parameters were measured *in-situ* including pH, salinity, water temperature, electrical conductivity, and total dissolved solids (TDS) using YSI 600 XLM Sondes (YSI Inc., Yellow Springs, OH). Secchi disk depth (SDD) was measured with a secchi disk. All water samples were stored in 1-L acid-cleaned plastic bottles, held on ice packs, and transported to the laboratory as soon as possible. In the laboratory, water samples were stored at 4 °C in a refrigerator, and analyzed within 2 days.

2.2. Water quality measurements

Water samples were analyzed for DOC concentration on a Shimadzu TOC Analyzer (680 °C) in the laboratory. Total nitrogen (TN) and total phosphorus (TP) were determined spectrophotometrically after digestion of the samples with alkaline potassium persulfate (Clesceri et al., 1998). Chlorophyll-a (*Chla*) concentration was obtained through extraction of a filtered sample (0.45 μm Whatman GF/F) with acetone solution (90%), and measured with a Shimazdu UV-2600 PC spectrophotometer (Jeffrey & Humphrey, 1975). Total suspended matter (TSM) was measured gravimetrically as described in Zhao et al. (2016).

2.3. CDOM absorption measurements and indices

In the laboratory, water samples were filtered through a 0.7 μm precombusted Whatman GF/F filter, and then through a 0.22 μm Millipore membrane cellulose filter. CDOM absorption spectra were determined using a Shimadzu UV-2600PC UV–Vis spectrophotometer, fitted with a 1-cm quartz cuvette, in the spectral region from 200 to 800 nm (1 nm interval). CDOM spectra for Milli-Q water were used as a reference. The CDOM absorption coefficient $a_{(\lambda)}$ was computed according to Eq. (1):

$$a_{(\lambda)} = 2.303A_{(\lambda)}/L \quad (1)$$

where L is the cuvette length (m), and $A_{(\lambda)}$ the measured optical density.

$$a(\lambda) = a(\lambda_0)\exp[S(\lambda_0 - \lambda)] \quad (2)$$

where $a(\lambda)$ is the absorption coefficient at wavelengthλ, $a(\lambda_0)$ is the absorption coefficient at a reference wavelength (λ_0), and S is the spectral slope (Bricaud et al., 1995; Babin et al., 2003). In this study, the absorption coefficient $a_{CDOM}254$ was used as a proxy for CDOM relative concentration. S is calculated by fitting a linear model to the data over a wavelength range of 275 to 295 nm with Eq. (2). The slope at the range of 275–295 nm ($S_{275\text{-}295}$) was used to characterize the CDOM composition and infer its sources (Helms et al., 2008)

Specific UV absorbance at 254 nm ($SUVA_{254}$), defined as the absorbance at 254 nm divided by the DOC concentration (mg/L), was used as an index of DOM aromaticity, with high values of $SUVA_{254}$ indicating DOM with a high aromatic content and low values indicating DOM with a low aromatic content (Weishaar et al. 2003). The ratio (M) of CDOM absorption coefficient at 250 nm and absorption coefficient at 365 nm ($M = a_{CDOM}250{:}a_{CDOM}365$) reflects the relative molecular weight of the humic component of DOM, with decreased M indicating increased molecular size of CDOM (Jones et al., 1988).

2.4. CDOM fluorescence measurement and FRI analysis

CDOM fluorescence excitation-emission matrices (EEMs) were measured using a Hitachi F-7000 fluorescence spectrometer equipped with a 700-V xenon lamp. The excitation (Ex) and emission (Em) scanning ranges were 200–450 nm and 250–500 nm, respectively. The spectra were recorded at a scan rate of 2400 nm min^{-1} using excitation and emission slit bandwidths of 5 nm. EEMs of Milli-Q water blanks were subtracted to eliminate the water Raman scatter. The elimination of the inner-filter effect was performed by adjusting for CDOM absorbance at the corresponding wavelengths according to Eq. (2) (McKnight et al., 2001; Kothawala et al., 2014). Interpolation was used to remove

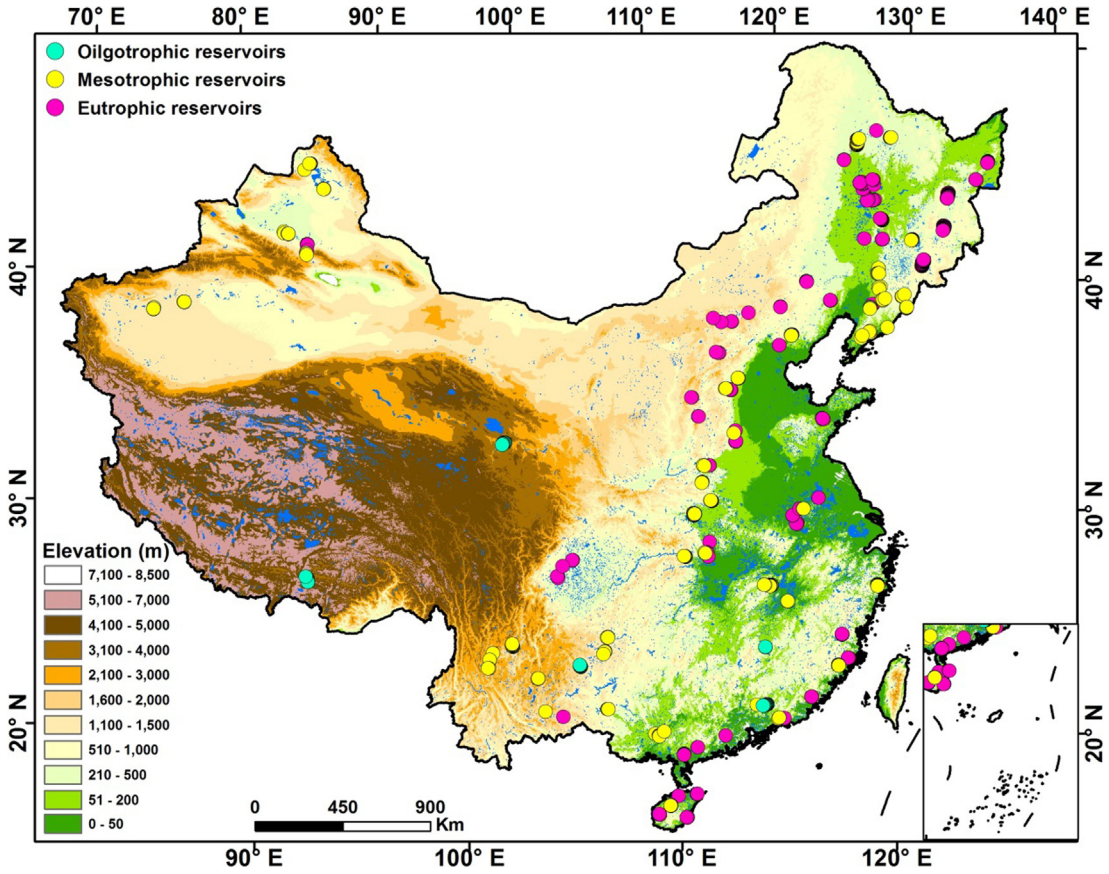

Fig. 1. The distribution of water sampling points across China, and the trophic status of sampled water reservoirs.

the effect of Rayleigh scattering (Stedmon and Bro, 2008).

$$Q_{cor} = Q_{obs} \times 10^{(A_{Ex}+A_{Em})/2} \quad (3)$$

where Q_{obs} and Q_{cor} represent fluorescence intensity of EEMs before and after calibration, respectively. The A_{Ex} and A_{Em} represent corrected absorbance at the corresponding excitation and emission wavelengths, respectively. The fluorescence was normalized to the integral of Raman signal to eliminate the effect daily variation in lamp intensity (Lawaetz and Stedmon, 2009).

Fluorescence regional integration (FRI) is a new quantitative approach to analyze the total wavelength-independent fluorescence intensity data based on EEM spectra (Chen et al., 2003; Sun and Mopper, 2016). EEM maps were divided into five regions: Q_1 (Ex 200–250 nm, Em 250–330 nm) tyrosine-like protein, Q_2 (Ex 200–250 nm, Em 330–350 nm) tryptophan-like protein, Q_3 (Ex 200–250 nm, Em 350–500 nm) fulvic acid-like organics, Q_4 (Ex 250–280 nm, Em 250–380 nm) microbial by-products, and Q_5 (Ex 280–400 nm, Em 380–500 nm) humic acid-like organics (Chen et al., 2003). The integral volume (Q_i) can be expressed as follows:

$$Q_i = \sum_{Ex}\sum_{Em} I(\lambda_{Ex}\lambda_{Em})\Delta\lambda_{Ex}\Delta\lambda_{Em} \quad (4)$$

where $I(\lambda_{Ex}\lambda_{Em})$ is the fluorescence intensity at each excitation–emission wavelength pair. $\Delta\lambda_{Ex}$ is the internal excitation wavelength (taken as 5 nm), $\Delta\lambda_{Em}$ is the internal emission wavelength (taken as 5 nm). The sum of the fluorescence intensities of FRI-divided FDOM components represent Q_T (unit: nm). The humification index (HIX) represents the ratio of allochthonous fluorescence intensity $Q_{3\&5}$ to that of the autochthonous fluorescence intensity $Q_{1\&2\&4}$ (Bilal et al., 2010).

The percentage of fluorescence response in a specific region (P_i = 1, 2, 3, 4, 5) was calculated as following:

$$P_i = Q_i/Q_T \times 100\% \quad (5)$$

2.5. Index of trophic state

The trophic state assessment of reservoirs was based on the modified Carlson's trophic state index (TSI_M) (Aizaki, 1981). This index was calculated using the three limnological parameters of chlorophyll *a* (*Chla*, μg/L), Secchi disk depth (SDD, m) and total phosphorus (TP, μg/L), according to the following equations:

$$TSI_M(Chla) = 10(2.46 + \frac{\ln Chla}{\ln 2.5}) \quad (6)$$

$$TSI_M(SDD) = 10(2.46 + \frac{3.69 - 1.53\ln SDD}{\ln 2.5}) \quad (7)$$

$$TSI_M(TP) = 10(2.46 + \frac{6.71 + 1.15\ln TP}{\ln 2.5}) \quad (8)$$

$$TSI_M = 0.297TSI_M(SDD) + 0.54 \times TSI_M(Chla) + 0.163 \times TSI_M(TP) \quad (9)$$

TSI_M results range from 0 to 100 and provide a scale to rate the trophic state of the reservoirs: $0 < TSI_M \leq 30$ oligotrophic; $30 < TSI_M \leq 50$ mesotrophic; $50 < TSI_M$ eutrophic.

2.6. The assessment of TSI_M model based on HIX

This study used an empirical approach for estimating TSI_M. The water samples were recorded and numbered from 1 to n (with n = 536) based on TSI_M values from low to high. According to the ranking order of the sampling, one sample was extracted at each of the two samples interval. The extracted 1/3 samples were used for model validation, while the others for model calibration. The correlation analysis between TSI_M and HIX was implemented. The coefficient of determination (R^2), root mean square error (RMSE), and percentage root mean square error

(%RMSE) between the measured and predicted values were calculated to assess goodness-of-fit and validation accuracy. The RMSE and % RMSE were determined using Eqs. (10) and (11) (n is the number of samples). The index of agreement (d) was to reflect the degree to which the measured variate was accurately estimated by the simulated variate. The index of agreement (d) was determined using Eq. (12), with P_i representing predicted TSI_M, M_i representing measured TSI_M, $\bar{M}$ representing the measured mean, P_i' representing the predicted TSI_M minus the measured mean, M_i' representing the measured TSI_M minus the measured mean. The index of agreement (d) varies between 0.0 and 1.0 where a computed value of 1.0 indicated perfect agreement between the measured and predicted values, and 0.0 connoted one of a variety of complete disagreements (Willmott, 1981).

$$\mathrm{RMSE} = \sqrt{\frac{1}{n} * \sum_{1}^{n} [TSI_M \ \ measured - TSI_M \ \ predicted]^2} \tag{10}$$

$$\%\mathrm{RMSE} = \mathrm{RMSE} * \frac{100 * n}{\sum_{1}^{n} TSI_M \ \ measured} \tag{11}$$

$$\mathrm{d} = 1 - \frac{\sum_{i=1}^{n} (P_i - M_i)^2}{\sum_{i=1}^{n} [|P_i'| + |M_i'|]^2} \tag{12}$$

2.7. Social and economic data and Statistical analyses

Social and economic data (wastewater and domestic sewage generation, fertilizer and pesticides use, cultivated land area, gross domestic product or GDP, population size) for the main cities within each reservoir's watershed was obtained from the National Bureau of Statistics for the period 2015–2017. Statistical analyses, including mean values, standard deviations, linear or non-linear regressions, and t-tests were performed using SPSS 16.0 software package (Statistical Program for Social Sciences, Chicago, IL). Difference was considered statistically significant when $p < 0.05$. Mapping of sampling sites was conducted using ArcGIS 10.1 (Environmental Systems Research Institute, Redlands, CA).

3. Results

3.1. Biogeochemical characteristics and trophic state

The sampled reservoirs had a wide range of trophic status as illustrated by the variations in nutrients and *Chla* (Table 1). The average concentration of DOC, SDD, *Chla* and TN, TP in the eutrophic reservoirs was noticeably higher than in the oligotrophic and mesotrophic reservoirs (Table 1). The difference in DOC concentration (and other water chemical parameters) among reservoirs of different trophic status was statistically significant ($p < 0.001$). Among the three trophic states of reservoirs, mean DOC concentration ranged from 1.56 to 7.17 mg L^{-1}. Similarly, the mean TP and TN concentration exhibited significant trophic variability, ranging from 0.03 to 0.15 mg P L^{-1} and 0.91 to 2.98 mg N L^{-1} respectively (Table 1). The range for *Chla* concentration was 1.02 to 46.62 μg L^{-1} for all reservoirs. The differences of TN, TP, *Chla* and SDD among the three trophic gradients of reservoirs were all significant ($p < 0.01$). The trophic states index (TSI_M) covered a wide range from 12 to 78. In total, our dataset included reservoirs with a wide range of trophic states, again suggesting that the data collected encompass conditions likely to be found in water reservoirs across China.

Table 1
Mean values of water quality parameters in reservoirs of different trophic states.

Trophic state	N	SDD (m)	*Chla* (μg/L)	DOC (mg/L)	TN (mg/L)	TP (mg/L)
Oligotrophic	42	5.72	1.02	1.56	0.91	0.03
Mesotrophic	251	3.66	3.52	2.64	1.67	0.05
Eutrophic	236	0.76	46.62	7.17	2.98	0.15

3.2. CDOM absorption and FDOM characteristics

3.2.1. CDOM characteristics

The $a_{CDOM}254$ ranged from 2.21 m^{-1} to 91.29 m^{-1} among the sampled reservoirs, and the mean $a_{CDOM}254$ showed an increasing trend from oligotrophic, mesotrophic, to eutrophic reservoirs, respectively (Fig. 2, Table S1). The $a_{CDOM}254$ values were significantly different among reservoirs of different trophic status ($p < 0.01$). The mean $S_{275\text{-}295}$ for oligotrophic, mesotrophic and eutrophic reservoirs was 27.2 μm, 20.6 um and 20.1 μm, respectively (Fig. 2). The $SUVA_{254}$ ranged from 2.98 to 4.60 L/mg m (Fig. 2). The mean value of M (related to the molecular weight of humic materials) decreased from 16.13 to 6.92 with increasing trophic state ($p < 0.01$). From oligotrophic to mesotrophic, $S_{275\text{-}295}$ increased significantly ($p < 0.01$), while from mesotrophic to eutrophic status, $S_{275\text{-}295}$ was nearly invariant. A similar but inverse trend was found with regard to $SUVA_{254}$ (Table S1). The significant changes from oligotrophic to mesotrophic and slight changes of $S_{275\text{-}295}$, M and $SUVA_{254}$ from mesotrophic to eutrophic indicated that, in the oligotrophic reservoirs, CDOM was predominantly derived from autochthonous sources, while the mesotrophic and eutrophic reservoirs have relatively high proportions of CDOM derived from allochthonous sources and exhibiting large molecular weight.

3.2.2. FRI-FDOM components

In this study, the FRI-based EEMs in different trophic reservoirs of China were analyzed to document trends in CDOM fluorescence characteristics about trophic status. The excitation-emission area volumes Q_i and P_i (i = 1, 2, 3, 4, and 5) were proportional to the total fluorescence intensity and the relative contribution of the five different components to the total fluorescence intensity. The examples of EEM fluorescence spectra from Yamdrok Lake (oligotrophic), Xiaolangdi Reservoir (mesotrophic), Hamatong Reservoir (eutrophic) and Xiashan reservoir (hyper-eutrophic) were selected as representative of reservoirs in various trophic gradients, and the partition of the five fluorescence components based on FRI-EEM are shown in Fig. 3. The total fluorescence intensity (Q_T) ranged from 5.48×10^{10} nm to 4.51×10^{12} nm for all water samples, and the mean Q_T from oligotrophic, mesotrophic to eutrophic status was 1.32×10^{11} nm, 2.64×10^{11} nm and 6.04×10^{11}, respectively (Fig. 4a). The relative contribution of individual components to total fluorescence intensity differed among water reservoirs of different trophic status (Fig. 4b). It was found that, the Q_5 (humic-like) and Q_3 (fulvic-like) compounds were predominant in FDOM for all types of reservoirs. With increased trophic status, the percentage of Q_1 and Q_4 decreased, while the percentage of Q_3 and Q_5 increased significantly ($p < 0.01$). The mean humification index (HIX) from oligotrophic, mesotrophic to eutrophic reservoirs was in the order of 3.26, 8.08 and 8.76 (Fig. 4c).

3.3. CDOM optical properties versus social and biogeochemical factors

The CDOM absorption coefficient at 254 nm showed a strong correlation with TN ($R = 0.93$, $p < 0.05$) (Table 2), while there were weak correlations between CDOM absorption and *Chla* or TP ($p < 0.05$). TN, TP, cultivated land area and GDP all showed positive correlations with allochthonous CDOM fluorescent components (Q_3 and Q_5) ($p < 0.05$, *t*-test) (Table 2). However, *Chla*, sewage discharge, agricultural fertilizer and pesticide use, and urban population size had close relationships with autochthonous CDOM fluorescent components (Q_2 and Q_4) ($p < 0.05$, *t*-test) (Table 2). The relationships between DEM and CDOM absorption and FDOM were all significant ($p < 0.01$) (Fig. 5). According to data obtained from the National Meteorological

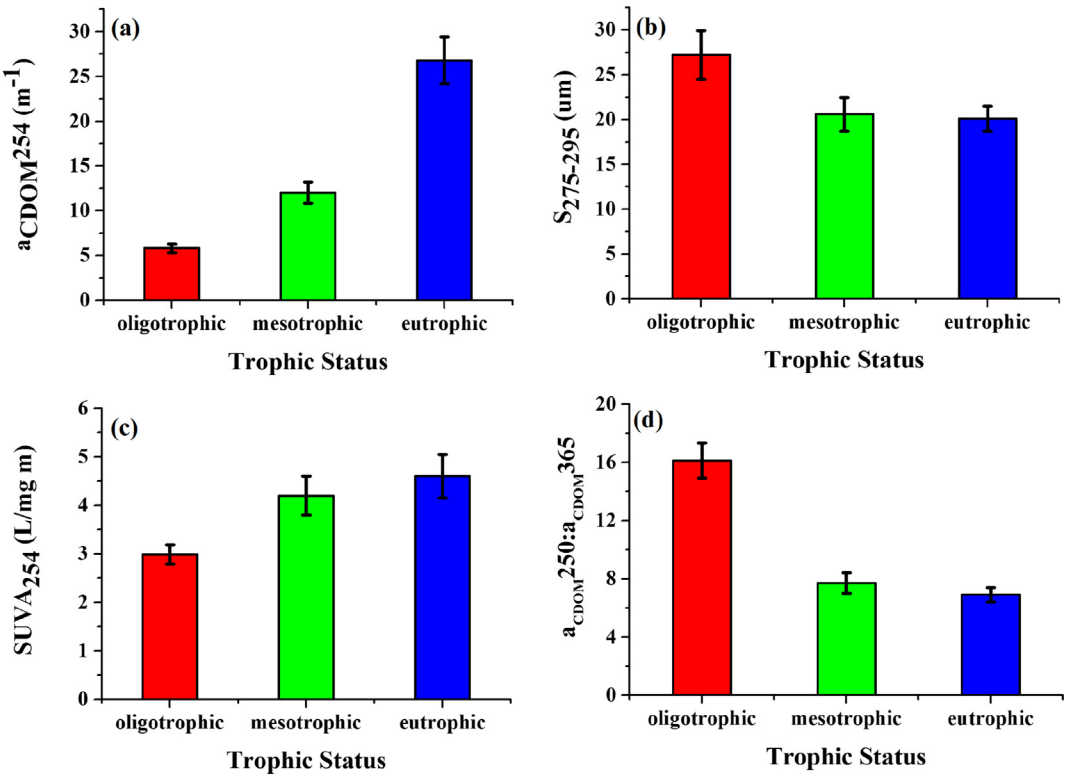

Fig. 2. The optical properties of CDOM (chromophoric dissolved organic matter) in Chinese water reservoirs of different trophic status. Figure panels: (a) CDOM absorption coefficients at 254 nm, (b) CDOM spectral slope ($S_{275-295}$) in the range of 275–295 nm (c) Specific UV absorbance at 254 nm ($SUVA_{254}$), (d) ratio of CDOM absorption coefficient at 250 nm and at 365 nm ($a_{CDOM}250:a_{CDOM}365$).

Information Center (http://data.cma.cn), solar radiation increased significantly with altitude ($R^2 = 0.41$, $p < 0.01$) (Fig. 5b). Although sunlight duration also arises with altitude, the relationship was weak ($R^2 = 0.18$, $p < 0.01$) (Fig. 5c). Nevertheless, $S_{275-295}$ increased significantly ($p < 0.01$) with elevation, suggesting photo-degradation could be an important process in the high-altitude reservoirs (Fig. 5d).

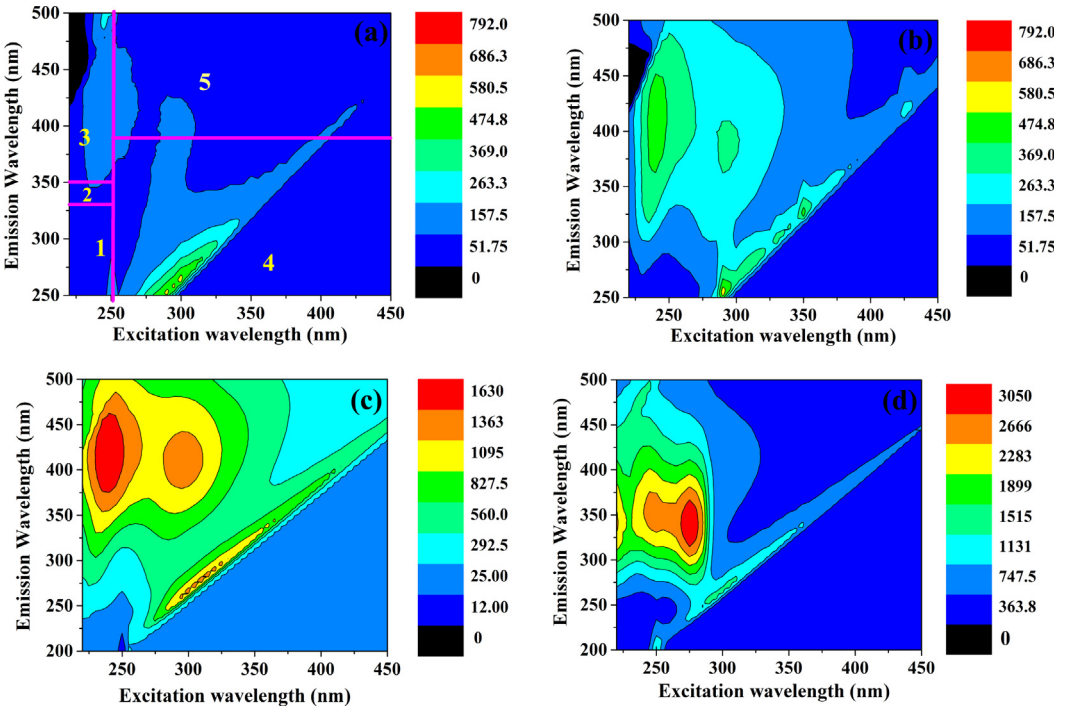

Fig. 3. CDOM fluorescence excitation-emission matrices (EEM) in relation to the trophic state of surface water bodies. Depicted here are examples of EEM_S for: (a) an oligotrophic lake (Yamdrok Lake), (b) a mesotrophic reservoir (Xiaolangdi Reservoir), (c) a eutrophic reservoir (Hamatong Reservoir), and (d) an hyper-eutrophic reservoir (Xiashan Reservoir).

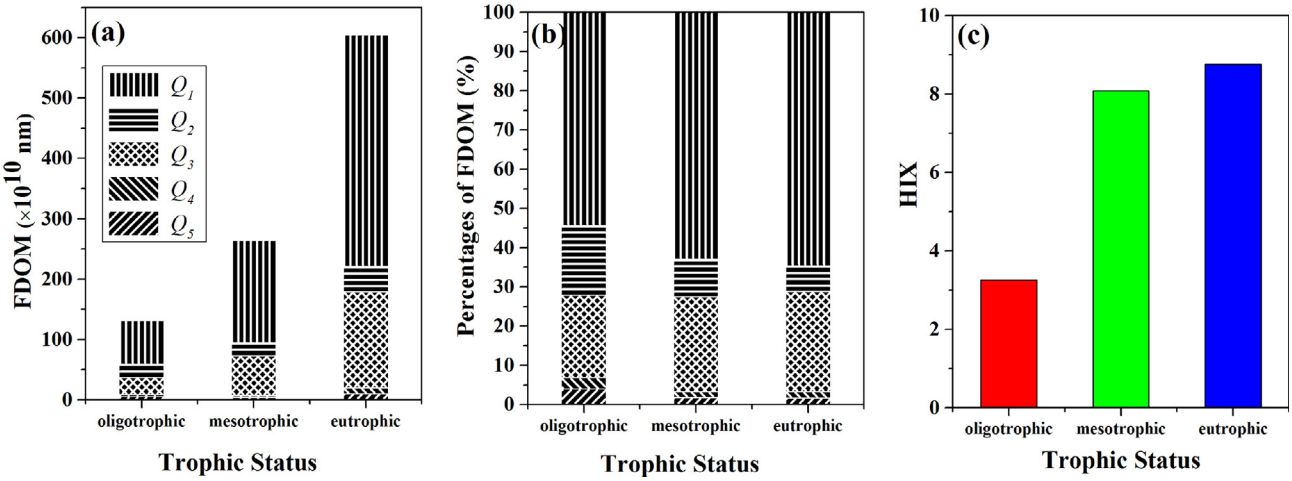

Fig. 4. (a) The fluorescence components of CDOM in water reservoirs of different trophic states, and (b) the relative percentage of individual components to the total fluorescence of CDOM. Components include Q1 (tyrosine-like protein), Q2 (tryptophan-like protein, Q3 (fulvic acid-like organics), Q4 (microbial by-products), and Q5 (humic acid-like organics) (Chen et al., 2003) and (c) the HIX for the reservoirs of different trophic status across China.

3.4. CDOM optical properties versus trophic states

There were weak relationships between individual TSI parameters (TSI_{Chla}, TSI_{TP}, TSI_{SDD}) and CDOM absorption ($p > 0.05$). But the synthetic TSI_M showed a significant relationship with CDOM absorption ($R^2 = 0.60$, $p < 0.01$), which suggested that CDOM absorption coefficients at 254 nm could be considered a potential indicator to evaluate the trophic status of reservoirs. The exponential regression equations between TSI_M and allochthonous CDOM fluorescent components (Q_3 and Q_5) were obtained with a relative moderate coefficient (Q_3: $R^2 = 0.48$, $p < 0.01$; Q_5: $R^2 = 0.45$, $p < 0.01$) (Fig. 6b–c). The TSI_M was negatively affected by CDOM absorption slope ($R = -0.21$, $p < 0.01$). In contrast, $SUVA_{254}$ increased as the TSI_M increased ($R = 0.19$, $p < 0.01$) (Table 3).

An important result of the present study is the significant correlations between TSI_M and HIX (coefficient of determination of 0.67 across Chinese reservoirs). This calibration model was applied to the remaining water samples for validation; the validation result is presented in Fig. 7. The %RMSE was 9.86% and the RMSE value of 4.73 and d is 0.92. Given these relationships (Fig. 6d and Fig. 7), we proposed a new classification whereby CDOM humification index can be used as a proxy for TSI_M (Table 4). The proposed classification would be as follows: oligotrophic state corresponding to $HIX \leq 4$ and $TSI_M \leq 30$; mesotrophic state with $4 < HIX \leq 12$ and $TSI_M \leq 50$; eutrophic state with $12 < HIX \leq 18$ and $TSI_M \leq 70$; hyper eutrophic status with $HIX > 18$ and $TSI_M > 70$.

4. Discussion

4.1. Water quality and social-economic factors

The higher determination coefficients (positive linear relationships) between TN and *Chla* ($p < 0.01$) than between TP and *Chla* ($p > 0.05$), suggested that nitrogen availability was probably the limiting factor of phytoplankton growth in the water reservoirs sampled for the present study. TN level is a critical water chemical parameter, and the strong relationships between TN and $a_{CDOM}254$ suggested that TN plays an important role in determining CDOM level in water reservoirs across China. The significant correlations between $a_{CDOM}254$ and TP, *Chla* indicated that the CDOM sources are also related to phosphorus inputs and phytoplankton activities. The correlations between CDOM absorption and urban population size indicated that anthropogenic activities, to some extent, are important contributors to the CDOM pool in the water reservoirs. This interpretation would be in agreement with a previous study in lakes from the Yungui region (Zhang et al., 2010). The strong correlation between TN and Q_T, further indicated that the fluorescent CDOM was dominated by organic nitrogen-containing compounds, especially terrestrial humic-like (Q_5) and fulvic-like (Q_3) substances. The linear correlation between humic-like component of FDOM (Q_5) and TN can be attributed to the nitrogen composition of the humic compounds present in water bodies (Zhao et al., 2017). The slope of the relationship between TN and Q_5 decreases from oligotrophic to eutrophic reservoirs (slope for oligotrophic: 0.07; mesotrophic: 0.035; eutrophic: 0.03); that pattern also indicated a connection between the relative abundance of large humic-like molecules and organic nitrogen level in the water reservoirs investigated.

Table 2
Correlation coefficients for the relationships between CDOM properties and socio-economic factors.

Parameters	Q_1	Q_2	Q_3	Q_4	Q_5	Q_T	$a_{CDOM}254$
Chla	−0.047	0.397*	0.398	0.782*	0.479	0.470	0.368*
TN	0.245	0.736	0.932*	0.935*	0.963**	0.961**	0.929*
TP	0.132	0.249	0.754*	0.181	0.811*	0.391	0.381*
Wastewater	−0.536	−0.088	0.133	0.665*	0.280	0.244	0.108
Domestic sewage	−0.359	0.310*	0.130	0.441*	0.779	0.411	0.289
Fertilizer	−0.408	0.135	0.582	0.914*	0.666	0.645	0.481
Pesticides	−0.196	0.362	0.635	0.957*	0.731	0.711	0.594
Cultivated land	−0.048	0.398	0.907*	0.821	0.923*	0.915*	0.851
GDP	−0.274	0.206	0.336*	0.792	0.449*	0.427*	0.302*
Population	−0.013	0.180*	−0.042	0.364*	−0.011	−0.004	−0.112

Note: *$p < 0.05$, **$p < 0.01$.

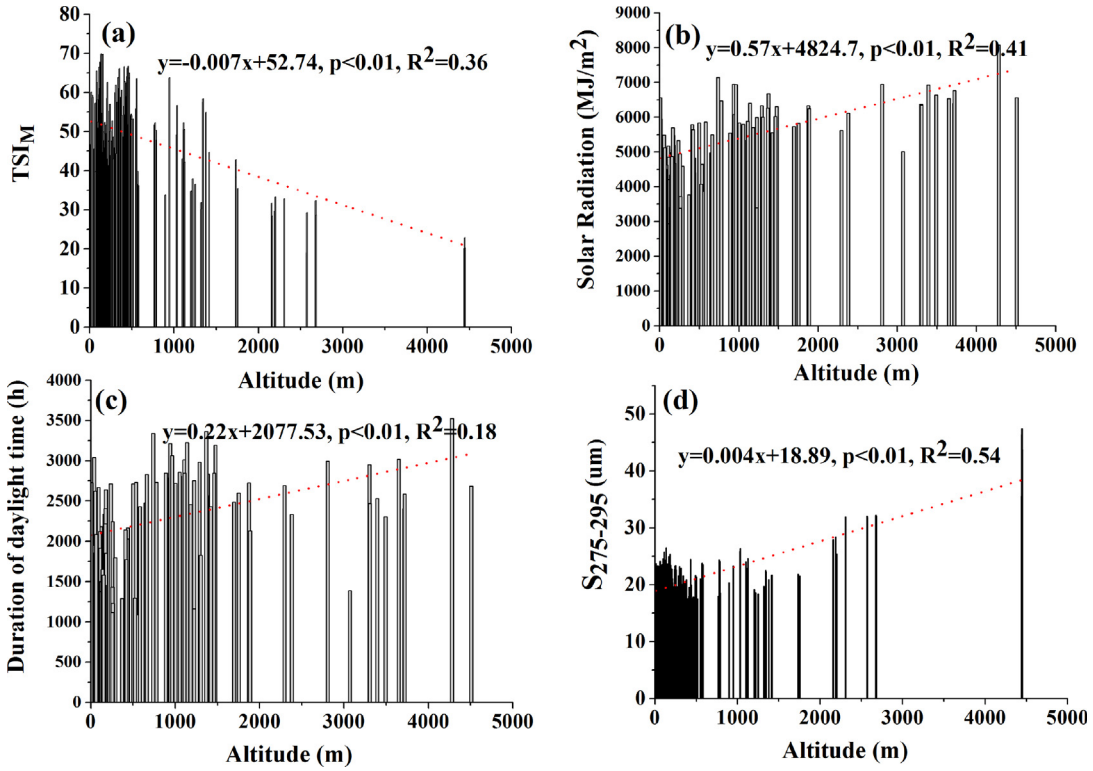

Fig. 5. Relationships between altitude and a) trophic state index (TSI_M) of water reservoirs, b) solar radiation, c) duration of sunlight, and d) CDOM spectral slope ($S_{275\text{-}295}$) in the range of 275–295 nm.

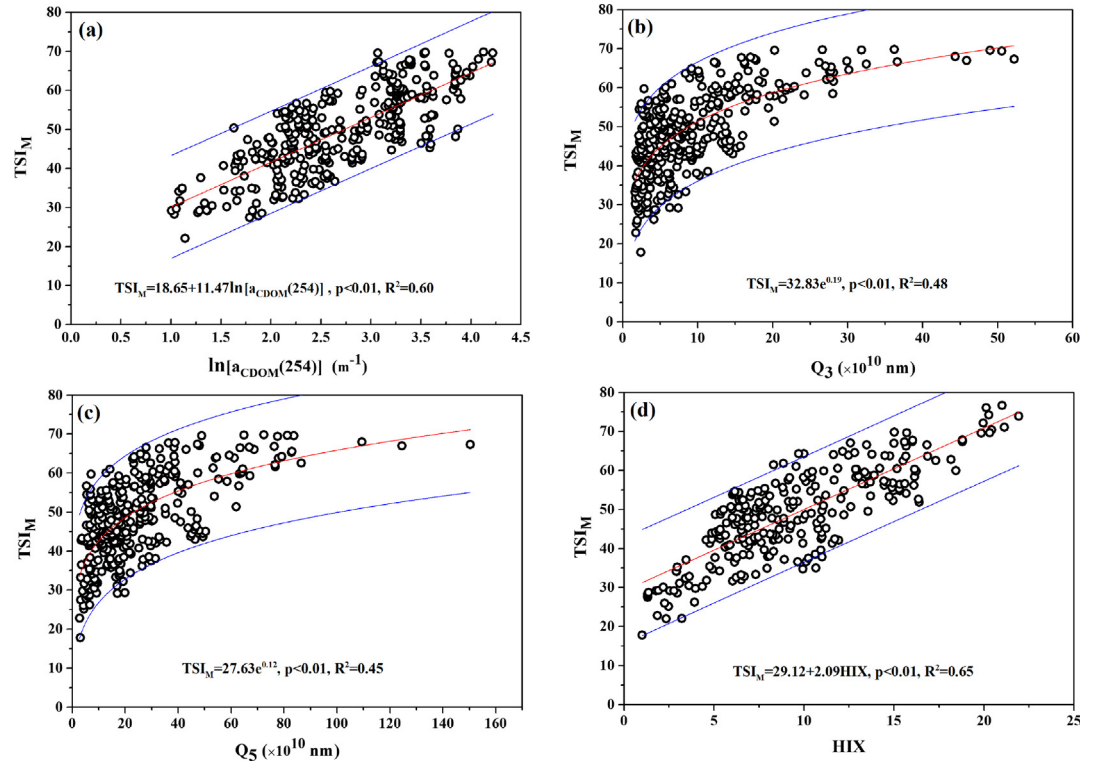

Fig. 6. Relationships between the trophic state index of water reservoirs (TSI_M) and CDOM optical and fluorescence parameters. Graph panels are: (a) TSI_M vs ln $a_{CDOM}(254)$; (b) TSI_M vs Q_3; (c) TSI_M vs Q_5; (d) TSI_M vs HIX. (The area between two blue lines indicates the 95% prediction interval around the red regression line). (For interpretation of the references to colour in this figure legend, the reader is referred to the web version of this article.)

Table 3
Correlation coefficients for the relationships between CDOM absorption, fluorescence properties of CDOM and modified trophic state index (TSI_M).

	Q_1	Q_2	Q_3	Q_4	Q_5	$a_{CDOM}254$	$S_{275-295}$	$SUVA_{254}$	ALT	TSI_M	HIX
Q_1	1	0.96**	0.61**	0.97**	0.56**	0.15**	0.11*	−0.11*	−0.01	0.20**	−0.17**
Q_2		1	0.72**	0.96**	0.67**	0.27**	0.10	−0.11*	−0.08	0.31**	−0.07
Q_3			1	0.64**	0.94**	0.69**	0.05	−0.01	−0.23**	0.69**	0.32**
Q_4				1	0.60**	0.16**	0.07	−0.08	−0.08	0.21*	−0.13**
Q_5					1	0.71**	−0.01	−0.01	−0.26**	0.67**	0.46**
$a_{CDOM}254$						1	0.02	0.19**	−0.20**	0.53**	0.50**
$S_{275-295}$							1	−0.43**	0.58**	−0.21**	−0.25**
$SUVA_{254}$								1	−0.29**	0.19*	0.22**
DEM									1	0.56**	−0.26**
TSI_M										1	0.81**
HIX											1

Note: *p < 0.05, **p < 0.01.
ALT: altitude.

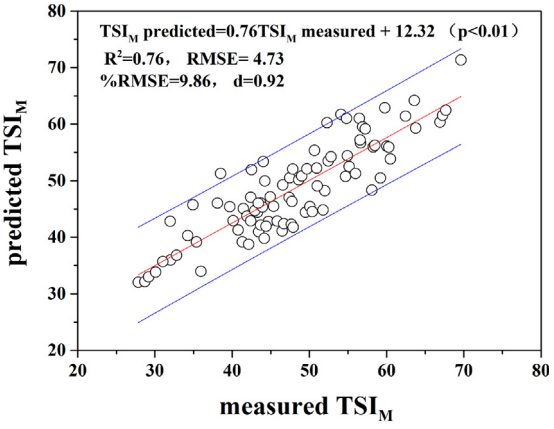

Fig. 7. Validation results of the TSI_M model through comparison of measured TSI_M and predicted TSI_M of water reservoirs. (The area between two blue lines indicates the 95% prediction intervals around the red regression line). (For interpretation of the references to colour in this figure legend, the reader is referred to the web version of this article.)

Table 4
Trophic state classification of water reservoirs across China based on the modified trophic state index (TSI_M) and the humification index of CDOM (HIX).

Indices	Trophic status			
	Oligotrophic	Mesotrophic	Eutrophic	Hyper-eutrophic
TSI_M	$TSI_M \leq 30$	$30 < TSI_M \leq 50$	$50 < TSI_M \leq 70$	$TSI_M > 70$
HIX	$HIX \leq 4$	$4 < HIX \leq 12$	$12 < HIX \leq 18$	$HIX > 18$

The correlations between *Chla* and Q_4 (Q_2) indicated that phytoplankton activities are related to autochthonous fluorescent components. The significant correlation between TP and Q_5 (Q_3) indicated that phosphorus is an important source for allochthonous fluorescent components. Previous studies had shown that the concentration of nitrogen and phosphorus in drainage waters during the rainy season can be much higher than in other months of the year (Zinabu, 2002; Chen et al., 2010). With expected changes in the global climate (heavy rainstorms, high water temperature), the impact of extreme weather events on water-quality could exacerbate in some world regions (Michalak, 2016). Therefore, in the future studies, we will carry on more fieldtrips to discuss the seasonal impact on CDOM and FDOM in details.

The positive correlation between industrial wastewater discharge and Q_4 of microbial protein-like components likely reflect stimulation of microbial activity from organic materials discharged from industrial and other anthropogenic sources. Microbial by-products may have contributed to the protein-like fluorescent compounds revealed by the FRI-EEM analysis (Yang et al., 2007). The large industrial facilities and wastewater outlets upstream of some of the reservoirs are potential contributors to increase in bacteria-derived DOM. The positive correlation between domestic sewage discharge and tryptophan-like components Q_2 observed in the present study is similar to the results of Wang et al. (2012) who interpreted the abundance of a tryptophan-like component as an indicator of intensive anthropogenic activities and microbial degradation of exogenous waste. Other studies have reported strong tryptophan-like fluorescence intensities in aquatic systems impacted by urban activities including discharge of residential sewage and animal farm wastes (Hong et al., 2005; Yang et al., 2007; Zhou et al., 2018). In addition, the relationships between urban population size and microbial protein-like components indicated that human activities might have resulted in high load of household sewage that fueled phytoplankton growth and degradation of dead biomass by resident microbes (Stedmon and Bro, 2008; Williams et al., 2010; Yamashita et al., 2008; Yao et al., 2011).

The strong correlation between cropland area and Q_3, Q_5 indicated that land disturbance during farming activities can be a significant driver of terrestrial CDOM input into the water reservoirs. Supporting that mechanism is the significant correlation observed between GDP and the allochthonous FDOM components Q_3 and Q_5. The correlations between agricultural input (fertilizers, pesticides) and the abundance of microbial protein-like compounds further underscore the influence of non-point agricultural pollution on nutrients enrichment, phytoplankton growth and intensification of the eutrophication phenomenon in the water reservoirs. Moreover, previous studies have noted that pesticides can be photo-chemically transformed in wetland waters (Zeng and Arnold, 2013) with CDOM as intermediates reaction products (Young et al., 2013). Further investigations are needed to explore possible linkages between the photochemical transformation of pesticides and the optical properties of CDOM in inland waters, and especially water reservoirs in agricultural landscapes.

4.2. The impact of altitude on reservoir CDOM

Previous studies have reported that the inherent optical properties of CDOM in natural waters can significantly affected by altitude and direct solar radiation (Morris 2009; Morel and Bélanger 2006). Zhang et al. (2010) reported that altitude negatively affected CDOM absorption in lakes in the Yungui Plateau. Our results showed that, with increased altitude, both the CDOM absorption at 254 nm and the allochthonous FDOM components Q_3 and Q_5 significantly decreased ($p < 0.01$) (Table 3). Sobek et al. (2007) also found a significant negative correlation between altitude and DOC concentration based on a large database of 7514 lakes from all over the world. Altitude could affect CDOM properties through decreased human activity, increased photochemical degradation, and decreased terrestrial CDOM input due

to reduced terrestrial productivity and catchment area in high-altitude regions (Zhang et al., 2010). The high-altitude reservoirs receive higher solar radiation than reservoirs located in lowland areas (Nima et al., 2016). As reported for the large and shallow Lake Taihu, prolonged water retention time and high UV light penetration could enhance the photo-degradation of terrestrially-derived humic-rich CDOM (Zhang et al., 2013; Shi et al., 2014). In our study, the decrease in CDOM absorption, fulvic-like components, and humic-like components also indicated that high exposure of CDOM to solar radiation in high-altitude water reservoirs may have resulted in photo-induced degradation of CDOM. Although the R^2 of the correlation between altitude and daylight time is low, the high coefficient R^2 for the correlation between altitude and solar radiation implied the process of photo-degradation of CDOM is more related to solar radiation intensity rather than the duration of daylight. The positive correlations between altitude and $S_{275\text{-}295}$, and the negative correlations between altitude and $SUVA_{254}$ could further support the above interpretation. A similar mechanism was invoked to explain CDOM characteristics in high-latitude alpine lakes receiving high solar UV fluxes, causing alterations in DOM composition and an abundance of compounds with low aromaticity (Sommaruga et al., 1999; Sommaruga, 2001). Similar observations were made in the US Cascade Mountains with an elevation range of 600 to > 2000 m (Nelson, 1991). The present study adds to our existing knowledge on that topic and the need to increase our understanding of the role of UV radiation on C chemistry in high-altitude water bodies round the globe.

The FDOM in reservoirs was predominantly associated with fulvic and humic acids, which explained the low correlation between autochthonous FDOM components (Q_1, Q_2, and Q_4) and altitude. Another possible reason for the lower correlation between these variables could be the rapid photo-degradation of algal-derived CDOM in deep waters from high-altitude water reservoirs (Johannessen et al., 2007; Hulatt et al., 2009). This interpretation would be consistent with prior studies that showed a stronger correlation between CDOM absorption and the humic-like peak than between CDOM absorption and the protein-like peak (Kowalczuk et al., 2010). In terms of allochthonous FDOM components, the decreasing rate (slope) of humic-like component Q_5 ($Q_5 = -5\ln(\text{altitude}) + 50$, $p < 0.01$) was higher than that of fulvic-like acids Q_3 ($Q_3 = -2\ln(\text{altitude}) + 20$, $p < 0.01$). This observation suggests that the loss of fluorescent humic-like components is significantly higher than that of fulvic-like components. It is consistent with a previous study which considered that humic acid is the primary target of DOM photo-degradation in natural waters (Wu et al., 2005). In surface waters, photo-degradation of the humic acid fraction is significantly greater than that of the fulvic acid fraction. It follows that fulvic acid is photolytically more stable than humic-like materials of CDOM in aqueous systems with long water residence time (Wu et al., 2005). It has been speculated that the high photolability of humic-like components could be related to their sensitivity to pH or the high production rate of H_2O_2 upon irradiation (Mostofa et al., 2009). Additional research is clearly needed to elucidate the underlying drivers of CDOM photo-degradation in natural waters.

The effect of altitude on CDOM properties and composition can be indirectly connected to trophic state due to the effects of altitude on nutrient input and on human activity (Norsang et al., 2014; Nima et al., 2016; Song et al., 2019). In addition, regions of high altitude are often characterized by limited vegetation growth, low cropland acreage, and low GDP. The relationship between altitude and TSI_M (Fig. 5a) illustrated that trend, and showed low primary productivity and low human disturbance in the watersheds draining into the high-altitude reservoirs. These observations are in agreement with the results of Zhang et al. (2010). The trend also suggested a possible co-variation between trophic state and altitude with both factors affecting CDOM concentration and composition. The significant positive correlation between altitude and $S_{275\text{-}295}$ ($p < 0.01$) (Table 3) indicated that the proportion of humic acids tends to decrease with high latitude due to decrease in terrestrial productivity (resulting in low terrestrial CDOM input). The negative correlation between altitude and $SUVA_{254}$ also implies that the aromaticity and molecular weight of CDOM also decreased ($p < 0.01$) (Table 3). It indicated that altitude indeed affects the sources and composition of CDOM to some extent.

4.3. Trophic gradients versus CDOM absorption and fluorescence

Past studies relating bio-optical parameters such as *Chla*-specific absorption coefficient and trophic status have been reported in oceanic waters (Oubelkheir et al., 2005; Brotas et al., 2013). For inland waters, however, few studies have focused on the relationship between CDOM absorption coefficient and composition, and TSI (Zhang et al., 2010). Using a comprehensive dataset from several lakes in China, Zhang et al. (2018) noted a parallel increase between CDOM absorption and trophic state. However, that dataset only included lakes in the eastern lake region and the Yungui lake region of China. Very few studies have examined the relationships between CDOM and TSI_M for the whole country, and to our knowledge no prior attempt has been made for the country's water reservoirs. Our study is perhaps the first that has attempted that examination. Indeed, as has been reported for lakes, our results have shown strong relationships between the modified trophic states index TSI_M and ln-transformed $a_{CDOM}(254)$, suggesting that the trophic state of water reservoirs can be predicted from CDOM absorption. We further demonstrated that the trophic state of reservoirs can also be derived from the humification index (HIX) of FDOM (Fig. 6a–d). Our results further indicated that CDOM composition was significantly different between reservoirs of different trophic states. Specifically, CDOM in the high trophic state reservoirs tends to be dominated by high molecular weight compounds than CDOM from oligotrophic reservoirs (Fig. 2b). Few past studies have investigated CDOM absorption coefficients and composition as a function of the trophic state of surface water (Zhang et al., 2010; Mladenov et al., 2011; Liu et al., 2014; Brandão et al., 2016; Zhang et al., 2018). For example, the hyper-eutrophic Pampulha Reservoir ($S_{275\text{-}295}$: 20 μm^{-1}) had a lower spectral slope than the oligotrophic Lake Dom Helvecio ($S_{275\text{-}295}$: 30 μm^{-1}). Conversely, and similar to our results (Fig. 2a), the CDOM absorption coefficients of oligotrophic lakes were markedly lower than those of lakes and reservoirs with higher trophic status (Zhang et al., 2010; Mladenov et al., 2011; Liu et al., 2014; Zhang et al., 2018).

The large range of trophic states exhibited by the water reservoirs included in the present study provided a unique opportunity to examine general trends in CDOM absorption variability in relation to the trophic gradient of aquatic ecosystems. However, it is important to recognize the limitations of the data presented. Due to logistical and financial constraints, factors such as land use, hydrology, seasonal variability were not systematically investigated (Wilson and Xenopoulos, 2009). Yet, in the context of a changing global climate, it is important for future studies to examine the significance of these hydro-climatic factors on the source and composition of CDOM in aquatic ecosystems.

The significant increase of humic-like components (Q_5) and fulvic-like component (Q_3) with increased trophic state (TSI_M) suggested that trophic state is affected by allochthonous fluorescence substances likely originated from the surrounding catchments, and increase in terrestrial fluorescent components. The autochthonous components (Q_2 and Q_4) were also significantly correlated ($p < 0.01$) (Table 3) with trophic states probably due to increased phytoplankton biomass in nutrient-rich and high trophic state reservoirs. Previous studies have reported similar increase of humic-like fluorescent substances with higher trophic state (Miller et al., 2009; Zhang et al., 2009). The percentage distribution of individual fluorescent components and the increased proportion of allochthonous fluorescent components (Q_3 and Q_5) indicated that CDOM fluorescence in the water reservoirs was dominated by humic-like components and that, with increased trophic state, allochthonous input from surrounding catchments formed a larger contribution to total fluorescence. This result is different from several previous studies that

have proposed that autochthonous protein-like components were predominant in lakes of the Yungui Plateau and other alpine and subalpine lakes (Hood et al., 2003; Miller et al., 2009; Zhang et al., 2010). These differences may due to the complex interactions of geological settings, land cover or land use, climatic conditions and intensity of anthropogenic disturbances in the area surrounding the reservoirs. All these factors can have variable impact on input and chemistry of allochthonous CDOM delivered to man-made water reservoirs.

4.4. Implications and uncertainty for TSI_M models based on HIX

The TSI_M provides an overall assessment of the ecological health of water reservoirs and can be used as a guide to make decisions regarding the monitoring and management of water quality in these important water bodies. Considering the relationships between CDOM and trophic state, some researchers have proposed to define lake trophic status using the nutrient-color paradigm to represent CDOM absorption (Williamson et al., 1999; Webster et al., 2008). Zhang et al. (2018) proposed to use CDOM absorption to classify the trophic status of lakes. Cunha et al. (2013) proposed a new TSI using TP and *Chla* concentrations. Webster et al. (2008) integrated TP concentration and colored DOC values to define trophic state using a diverse dataset of 1646 lakes. The significant correlation between HIX and TSI_M indicated that the allochthonous fluorescence sources increased with trophic state, and that intense eutrophication should be expected with increase in the humification of CDOM sources (Fig. 6d). A rise in terrestrial DOM input would also imply greater nutrients input from the catchment which in turn trigger phytoplankton growth and increased risk of hypoxia.

Many studies have shown that the trophic status is strongly dependent upon the input of nutrients organic matter (energy) from terrestrial ecosystems (Kissman et al., 2017; Beck et al., 2018). Here, based on strong relationships between HIX and chemistry of dissolved organic matter in freshwater reservoirs, we demonstrated for the first time a new approach to determine the trophic state of reservoirs using CDOM fluorescence characteristics. The traditional TSI calculation using *Chla*, SDD and TP does not fully account for the interactions among these parameters and for the influence of water color, especially for turbid inland waters (Zhu et al., 2011; Kutser, 2012). The fluorescence CDOM is easy to determine and is more sensitive than traditional water quality measurements. The distribution of CDOM fluorescence in water reservoirs can be made with handheld spectrometers, as well as with sensors on board of unmanned aerial vehicles and land-observing satellites, making it possible to continuously monitor changes in the trophic state of water reservoirs, many of which are sources of drinking water.

Our results are based on a large dataset encompassing reservoirs of a large range of trophic state. Therefore, our assessment model should be applicable to a wide range of inland water bodies within the study region. However, some errors or uncertainties are likely if the proposed classification is applied to oligotrophic and hyper-eutrophic reservoirs since few samples from oligotrophic and hyper-eutrophic systems were included in model development. System error during CDOM fluorescence measurement may also affect the accuracy of HIX to some extent. The model did not account for difference in geological settings, and seasonal variation in the chemistry of allocthonous CDOM input from terrestrial sources. Future studies should consider these limitations, and should endeavor to collect data from other eco-regions in order to build a more robust model for accurate determination of the trophic status of water reservoirs from the optical properties of CDOM.

5. Conclusions

The present study examined the optical characteristics of CDOM from 131 water reservoirs of different trophic state distributed across China. Based on strong relationships between the HIX of FDOM and the TSI_M of water reservoirs, the study demonstrated that the HIX of CDOM fluorescence can be used as a new classification index to express the trophic state of water reservoirs. This method highlights the linkage of trophic status and DOM optical characteristics, and provides an approach for rapid and continuous monitoring of the ecological integrity of water reservoirs. Future studies should examine the applicability and performance of that approach in other types of inland waters around the globe.

Declaration of Competing Interest

The authors declare that they have no known competing financial interests or personal relationships that could have appeared to influence the work reported in this paper.

Acknowledgements

This research was jointly supported by the Strategic Priority Research Program of the Chinese Academy of Sciences (XDA19070501), the National Natural Science Foundation of China (No. 41730104 and 41471293), and project of Science and Technology Development plan of Jilin Province of China (20170301001NY) and the “Hundred Talents Program” of the Chinese Academy of Sciences through a grant to Dr. Kaishan Song. The authors thank all staff and students for their considerable assistance with both field sampling and laboratory analysis.

Appendix A. Supplementary material

Supplementary data to this article can be found online at https://doi.org/10.1016/j.jhydrol.2019.06.028.

References

Aizaki, M., 1981. Application of modified Carlson's trophic state index to Japanese lakes and its relationships to other parameters related to trophic state (in Japanese with English summary). Res. Rep. Natl. Inst. Environ. Stud. Jpn. 23, 13–31.
Babin, M., et al., 2003. Variations in the light absorption coefficients of phytoplankton, nonalgal particles, and dissolved organic matter in coastal waters around Europe. J. Geophys. Res. Oceans 108 (C7).
Beck, K.K., Fletcher, M.-S., Kattel, G., Barry, L.A., Gadd, P.S., Heijnis, H., et al., 2018. The indirect response of an aquatic ecosystem to long-term climate-driven terrestrial vegetation in a subalpine temperate lake. J. Biogeogr. 45, 713–725.
Bilal, M., Jaffrezic, A., Dudal, Y., Le, G.C., Menasseri, S., Walter, C., 2010. Discrimination of farm waste contamination by fluorescence spectroscopy coupled with multivariate analysis during a biodegradation study. J. Agric. Food Chem. 58, 3093–3100.
Bowling, L.C., Zamyadi, A., Henderson, R.K., 2016. Assessment of in situ fluorometry to measure cyanobacterial presence in water bodies with diverse cyanobacterial populations. Water Res. 105, 22–33.
Brandão, L.P., Staehr, P.A., Bezerra-Neto, J.F., 2016. Seasonal changes in optical properties of two contrasting tropical freshwater systems. J. Limnol. 75 (3).
Bricaud, A., Babin, M., Morel, A., Claustre, H., 1995. Variability in the chlorophyll-specific absorption coefficients of natural phytoplankton: Analysis and parameterization. J. Geophys. Res. Oceans 100 (C7), 13321–13332.
Brotas, V., Brewin, R.J.W., Sa, C., Brito, A.C., Silva, A., Mendes, C.R., Diniz, T., Kaufmann, M., Tarran, G., Groom, S.B., 2013. Deriving phytoplankton size classes from satellite data: validation along a trophic gradient in the eastern Atlantic Ocean. Rem. Sens. Environ. 134 (5), 66–77.
Carlson, R.E., 1977. A trophic state index for lakes. Limniol. Oceanogr. 22, 361–369.
Carpenter, S.R., Cole, J.J., Kitchell, J.F., Pace, M.L., 1998. Impact of dissolved organic carbon, phosphorus, and grazing on phytoplankton biomass and production in experimental lakes. Limnol. Oceanogr. 43, 73–80.
Chen, W., Westerhoff, P., Leenheer, J.A., Booksh, K., 2003. Fluorescence excitation-emission matrix regional integration to quantify spectra for dissolved organic matter. Environ. Sci. Technol. 37 (24), 5701–5710.
Chen, X., Wo, F., Chen, C., Fang, K., 2010. Seasonal changes in the concentrations of nitrogen and phosphorus in farmland drainage and groundwater of the Taihu lake region of China. Environ. Monit. Assess. 169 (1–4), 159–168.
Clesceri, L.S., Greenberg, A.E., Eaton, A.D., 1998. Standard Methods for the Examination of Water and Wastewater, 20th ed. APHA, AWWA, and WEF, Washington, DC.
Cunha, D.G.F., Calijuri, M.D.C., Lamparelli, M.C., 2013. A trophic state index for tropical/subtropical reservoirs (TSI tsr). Ecol. Eng. 60 (6), 126–134.
Dunalska J., 2009, Variability of organic carbon forms in lake ecosystems of varying trophic state. Wyd. UWM Olsztyn, pp. 115. (in Polish with English summary).
Dunalska, J., 2011. Total organic carbon as a new index for monitoring trophic states in lakes. Oceanol. Hydrobiol. Stud. 40 (2), 112–115.
Han, B.P., 2010. Reservoir ecology and limnology in China: a retrospective comment. J Lake Sci 22, 151–160 (in Chinese with English summary).
Helms, J.R., Stubbins, A., Ritchie, J.D., Minor, E.C., Kieber, D.J., Mopper, K., 2008.

Absorption spectral slopes and slope ratios as indicators of molecular weight, source, and photobleaching of chromophoric dissolved organic matter. Limnol. Oceanogr. 53, 955–969.
Hong, H., Wu, J., Shang, S., Hu, C., 2005. Absorption and fluorescence of chromophoric dissolved organic matter in the Pearl River Estuary, South China. Mar. Chem. 97, 78–89.
Hood, E., McKnight, D.M., Williams, M.W., 2003. Sources and chemical character of dissolved organic carbon across an alpine/subalpine ecotone, Green Lakes Valley, Colorado Front Range, United States. Water Resour. Res. 39, 118.
Hulatt, C.J., Thomas, D.N., Bowers, D.G., Norman, L., Zhang, C., 2009. Exudation and decomposition of chromophoric dissolved organic matter (CDOM) from some temperate macroalgae. Estuar. Coast. Shelf Sci. 84, 147–153.
Jeffrey, S.W., Humphrey, G.F., 1975. New spectrophotometric equations for determining chlorophylls a, b, c1 and c2 in higher plants, algae and natural phytoplankton. Biochemie Und Physiologie Der Pflanzen 167 (2), 191–194.
Johannessen, S.C., Peña, M.A., Quenneville, M.L., 2007. Photochemical production of carbon dioxide during a coastal phytoplankton bloom. Estuar. Coast. Shelf Sci. 73, 236–242.
Jones, R., Salonen, K., De Haan, H., 1988. Phosphorus transformations in the epilimnion of humic lakes: abiotic interactions between dissolved humic materials and phosphate. Freshw. Biol. 19 (3), 357–369.
Kissman, C.E., Williamson, C.E., Rose, K.C., Saros, J.E., 2017. Nutrients associated with terrestrial dissolved organic matter drive changes in zooplankton: phytoplankton biomass ratios in an alpine lake. Freshw. Biol. 62, 40–51.
Kowalczuk, P., Cooper, W.J., Durako, M.J., Kahn, A.E., Gonsior, M., Young, H., 2010. Characterization of dissolved organic matter fluorescence in the South Atlantic Bight with use of PARAFAC model: Relationships between fluorescence and its components, absorption coefficients and organic carbon concentrations. Mar. Chem. 118, 22–36.
Kothawala, D.N., Stedmon, C.A., Müller, R.A., Weyhenmeyer, G.A., Köhler, S.J., Tranvik, L.J., 2014. Controls of dissolved organic matter quality: evidence from a large scale boreal lake survey. Glob. Change Biol. 20, 1101–1114.
Kratzer, C.R., Brezonik, P.L., 2010. A Carlson-type trophic state index for nitrogen in Florida lakes. Jawra J. Am. Water Resour. Assoc. 17 (4), 713–715.
Kutser, T., 2012. The possibility of using the Landsat image archive for monitoring long time trends in coloured dissolved organic matter concentration in lake waters. Rem. Sens. Environ. 123, 334–338.
Lawaetz, A.J., Stedmon, C.A., 2009. Fluorescence intensity calibration using the Raman scatter peak of water. Appl. Spectrosc. 63, 936–940.
Lee, E.-J., Yoo, G.-Y., Jeong, Y., Kim, K.-U., Park, J.-H., Oh, N.-H., 2015. Comparison of UVeVIS and FDOM sensors for in situ monitoring of stream DOC concentrations. Biogeosciences 12 (10), 3109–3118.
Liu, X., Zhang, Y., Shi, K., Zhu, G., Xu, H., Zhu, M., 2014. Absorption and fluorescence properties of chromophoric dissolved organic matter: implications for the monitoring of water quality in a large subtropical reservoir. Environ. Sci. Pollut. Res. 21 (24), 14078–14090.
McKnight, D.M., Boyer, E.W., Westerhoff, P.K., Doran, P.T., Kulbe, T., Andersen, D.T., 2001. Spectrofluorometric characterization of dissolved organic matter for indication of precursor organic material and aromaticity. Limnol. Oceanogr. 46, 38–48.
Michalak, A.M., 2016. Study role of climate change in extreme threats to water quality. Nature 535 (7612), 349–350.
Miller, M.P., Mcknight, D.M., Chapra, S.C., Williams, M.W., 2009. A model of degradation and production of three pools of dissolved organic matter in an alpine lake. Limnol. Oceanogr. 54, 2213–2227.
Mladenov, N., Sommaruga, R., Moralesbaquero, R., Laurion, I., Camarero, L., Dieguez, M.C., Camacho, A., Delgado, A., Torres, O., Chen, Z., 2011. Dust inputs and bacteria influence dissolved organic matter in clear alpine lakes. Nat. Commun. 2 (3), 405.
Morel, A., Bélanger, S., 2006. Improved detection of turbid waters from ocean color sensors information. Remote Sens. Environ. 102, 237–249.
Morris, D.P., 2009. Optical properties of water. In: Gene, E.L. (Ed.), Encyclopedia of Inland waters Oxford. Academic Press, Massachusetts, pp. 682–689.
Mostofa, K.M.G., Liu, C., Wu, F.C., Fu, P.Q., Ying, W.L., Yuan, J., 2009. Overview of key biogeochemical functions in lake ecosystem: impacts of organic matter pollution and global warming. In: Keynote Speech, Proceedings of the 13 th World Lake Conference Wuhan, China, 1–5 Nov 2009, pp. 59–60.
Nelson, P.O., 1991. Acidic deposition and aquatic ecosystems: Cascade mountains. In: Charles, D.F. (Ed.), Springer-Verlag, New York, pp. 531–563.
Nima, C., Hamre, B., Frette, Øyvind, Erga, S.R., Chen, Y.C., Zhao, L., et al., 2016. Impact of particulate and dissolved material on light absorption properties in a high-altitude lake in tibet, china. Hydrobiologia 768 (1), 63–79.
Norsang, G., Chen, Y.C., Pingcuo, N., Dahlback, A., Frette, Ø., Kjeldstad, B., Hamre, B., Stamnes, K., Stamnes, J.J., 2014. Comparison of ground-based measurements of solar UV radiation at four sites on the Tibetan Plateau. Appl. Opt. 53, 736–747.
Nürnberg, G.K., 2001. Eutrophication and Trophic State. LakeLine 21, 29–33.
Oubelkheir, K., Claustre, H., Sciandra, A., Babin, M., 2005. Bio-optical and biogeochemical properties of different trophic regimes in oceanic waters. Limnol. Oceanogr. 50 (6), 1795–1809.
Shi, K., Zhang, Y., Liu, X., Wang, M., Qin, B., 2014. Remote sensing of diffuse attenuation coefficient of photosynthetically active radiation in Lake Taihu using MERIS data. Remote Sens. Environ. 140, 365–377.
Smith, V.H., Schindler, D.W., 2009. Eutrophication science: where do we go from here? Trends Ecol. Evol. 24, 201–220.
Sobek, S., Tranvik, L.J., Prairie, Y.T., Kortelainen, P., Cole, J.J., 2007. Patterns and regulation of dissolved organic carbon: an analysis of 7,500 widely distributed lakes. Limnol. Oceanogr. 52 (3), 1208–1219.
Sommaruga, R., 2001. The role of UV radiation in the ecology of alpine lakes. J. Photochem. Photobiol. B: Biol. 62 (1–2), 35–42.
Sommaruga, R., Psenner, R., Schafferer, E., Koinig, K.A., Sommaruga-Wögrath, Sabine, 1999. Dissolved organic carbon concentration and phytoplankton biomass in high-mountain lakes of the austrian alps: potential effect of climatic warming on UV underwater attenuation. Arct. Antarct. Alp. Res. 31, 247–254.
Song, K., Shang, Y., Wen, Z., Jacinthe, P.-A., Liu, G., Lyu, L., Fang, C., 2019. Characterization of CDOM in saline and freshwater lakes across China using spectroscopic analysis. Water Res. 150, 403–417.
Stedmon, C.A., Bro, R., 2008. Characterizing dissolved organic matter fluorescence with parallel factor analysis: a tutorial. Limnol Oceanogr : Meth 6, 572–579.
Sun, L., Mopper, K., 2016. Studies on hydroxyl radical formation and correlated photoflocculation process using degraded wood leachate as a CDOM source. Front. Marine Sci. 2.
Vörösmarty, C.J., Green, P., Salisbury, J., Lammers, R.B., 2000. Global water resources: vulnerability from climate change and population growth. Science 289 (5477), 284–288.
Wang, Y., Li, X., Li, B.H., Shen, Z.Y., Feng, C.H., Chen, Y.X., 2012. Characterization, sources, and potential risk assessment of PAHs in surface sediments from nearshore and farther shore zones of the Yangtze Estuary. China. Environ Sci. Pollut. R 19, 4148–4158.
Webster, K.E., Soranno, P.A., Spence, C.K., Bremigan, M.T., Downing, J.A., Vaux, P.D., et al., 2008. An empirical evaluation of the nutrient-color paradigm for lakes. Limnol. Oceanogr. 53 (3), 1137–1148.
Weishaar, J.L., Aiken, G.R., Bergamaschi, B.A., Fram, M.S., Fujii, R., Mopper, K., 2003. Evaluation of specific ultraviolet absorbance as an indicator of the chemical composition and reactivity of dissolved organic carbon. Environ. Sci. Technol. 37 (20), 4702–4708.
Williams, C.J., Yamashita, Y., Wilson, H.F., Jaffé, R., Xenopoulos, M.A., 2010. Unraveling the role of land use and microbial activity in shaping dissolved organic matter characteristics in stream ecosystems. Limnol. Oceanogr. 55 (3), 1159–1171.
Williamson, C.E., Morris, D.P., Pace, M.L., Olson, A.G., 1999. Dissolved organic carbon and nutrients as regulators of lake ecosystems: resurrection of a more integrated paradigm. Limnol. Oceanogr. 44 (3), 795–803.
Willmott, C.J., 1981. On the validation of models. Phys. Geogr. 2 (2), 184–194.
Wilson, H.F., Xenopoulos, M.A., 2009. Effects of agricultural land use on the composition of fluvial dissolved organic matter. Nat. Geosci. 2, 37–41.
Wu, F.C., Mills, R.B., Cai, Y.R., Evans, R.D., Dillon, P.J., 2005. Photodegradation-induced changes in dissolved organic matter in acidic waters. Can. J. Fish. Aquat. Sci. 62, 1019–1027.
Yamashita, Y., Jaffé, R., Maie, N., Tanoue, E., 2008. Assessing the dynamics of dissolved organic matter (DOM) in coastal environments by excitation emission matrix fluorescence and parallel factor analysis (EEM–PARAFAC). Limnol. Oceanogr. 1900–1908.
Yang, F., Huang, Q., Li, J., Zhu, X., 2007. Chracterization of chromophoric dissolved organic matter in the Yangtze Estuary by absorption and fluorescence spectroscopy. Jesss 1, 55–60.
Yang, J., Yu, X., Liu, L., Zhang, W., Guo, P., 2012. Algae community and trophic state of subtropical reservoirs in southeast Fujian, China. Environ. Sci. Pollut. Res. 19 (5), 1432–1442.
Yao, X., Zhang, Y., Zhu, G., Qin, B., Feng, L., Cai, L., Gao, G., 2011. Resolving the variability of CDOM fluorescence to differentiate the sources and fate of DOM in Lake Taihu and its tributaries. Chemosphere 82, 145–155.
Young, R., Latch, D., Mawhinney, D., Nguyen, T.-H., Davis, J., Borch, T., 2013. Direct photodegradation of androstenedione and testosterone in natural sunlight: inhibition by dissolved organic matter and reduction of endocrine disrupting. Environ. Sci. Technol. 47, 8416–8424.
Zeng, T., Arnold, W.A., 2013. Pesticide photolysis in prairie potholes: probing photosensitized processes. Environ. Sci. Technol. 47, 6735–6745.
Zhang, Y., Liu, X., Wang, M., Qin, B., 2013. Compositional differences of chromophoric dissolved organic matter derived from phytoplankton and macrophytes. Org. Geochem. 55, 26–37.
Zhang, Y., van Dijk, M.A., Liu, M., Zhu, G., Qin, B., 2009. The contribution of phytoplankton degradation to chromophoric dissolved organic matter (CDOM) in eutrophic shallow lakes: Field and experimental evidence. Water Res. 43 (18), 4685–4697.
Zhang, Y., Zhang, E., Yin, Y., Dijk, M.A.V., Feng, L., Shi, Z., et al., 2010. Characteristics and sources of chromophoric dissolved organic matter in lakes of the yungui plateau, china, differing in trophic state and altitude. Limnol. Oceanogr. 55 (6), 2645–2659.
Zhang, Y., Zhou, Y., Shi, K., Qin, B., Yao, X., Zhang, Y., 2018. Optical properties and composition changes in chromophoric dissolved organic matter along trophic gradients: implications for monitoring and assessing lake eutrophication. Water Res. 131, 255–263.
Zhao, Y., Song, K., Li, S., Ma, J., Wen, Z., 2016. Characterization of CDOM from urban waters in Northern-Northeastern China using excitation-emission matrix fluorescence and parallel factor analysis. Environ. Sci. Pollut. Res. 23 (15), 15381–15394.
Zhao, Y., Song, K., Wen, Z., Fang, C., Shang, Y., Lv, L., 2017. Evaluation of CDOM sources and their links with water quality in the lakes of northeast china using fluorescence spectroscopy. J. Hydrol. 550.
Zhou, Y., Wen, H., Liu, J., Pu, W., Chen, Q., Wang, X., 2018. The optical characteristics and sources of chromophoric dissolved organic matter (CDOM) in seasonal snow of northwestern china. Cryosphere 1–58.
Zhu, W., Yu, Q., Tian, Y.Q., Chen, R.F., Gardner, G.B., 2011. Estimation of chromophoric dissolved organic matter in the Mississippi and Atchafalaya river plume regions using above-surface hyperspectral remote sensing (1978–2012). J. Geophys. Res. Oceans 116 (C2).
Zinabu, G.M., 2002. The effects of wet and dry seasons on concentrations of solutes and phytoplankton biomass in seven Ethiopian rift-valley lakes. Limnologica 32 (2), 169–179.